Energy, Mines and Resources Canada | Énergie, Mines et Ressources Canada

CANMET

Canada Centre for Mineral and Energy Technology | Centre canadien de la technologie des minéraux et de l'énergie

EXAMINATION OF CORROSION PROBES FROM A LABORATORY-SCALE CIRCULATING FLUIDIZED BED COMBUSTOR

J.B. GILMOUR
CORROSION SCIENCE SECTION

FEBRUARY 1987

PHYSICAL METALLURGY RESEARCH LABORATORIES

REPORT: PMRL 87-8(TR)

PHYSICAL METALLURGY RESEARCH LABORATORIES

REPORT: PMRL 86-8(TR)

EXAMINATION OF CORROSION PROBES FROM A LABORATORY-SCALE CIRCULATING FLUIDIZED BED COMBUSTOR

by

J.B. Gilmour

Corrosion Science Section

ABSTRACT

Six Type 304 stainless steel tubes that had been exposed in the combustion zone of a laboratory-scale circulating fluidized bed combustor (CFBC) in the Mineral Sciences Laboratory were examined for corrosive attack. All tubes had been exposed for about 125 h at 850°C; three while the combustor was fueled with vanadium-containing Syncrude coke, and three while it was fueled with Minto coal. Metallographic examination showed that all tubes had suffered intergranular sulphidation/oxidation on the bottoms where deposits formed during operation. The area and depth of attack were similar on all tubes. The tops of all tubes had negligible attack. The morphology of the intergranular attack was similar to that observed on austenitic alloys exposed in the bed of bubbling-bed atmospheric fluidized bed combustors (AFBC). There was no evidence that the vanadium in the Syncrude coke played a role in the corrosion.

LABORATOIRES DE RECHERCHE NE METALLURGIE PHYSIQUE

RAPPORT: PMRL 86-8(TR)

EVALUATION DE SONDES A CORROSION A PARTIR D'UN REACTEUR DE COMBUSTION EN LIT FLUIDISE CIRCULANT A ECHELLE LABORATOIRE

par

J.B. GILMOUR

RESUME

Six tubes de type 304 en acier inoxydable, qui ont été placées dans un réacteur de combustion en lit fluidisé circulant à céllule laboratoire, au laboratoire des sciences minérales ont été examinés en regard de leur résistance à la corrosion. Tous les tubes ont été exposés à une température de 850°C pendant environ 125 heures. Trois de ces tubes ont été exposés alors que le réacteur était alimenté avec de la coke "syncrude" contenant du vanadium, alors que les trois autres ont été exposés pendant que le réacteur était alimenté au charbon Minto. Un examen métallographique a montré que les six tubes ont souffert de sulfuration/oxydation intergranulaire dans la partie du fond, là où des dépôts se forment lors de l'opération. La superficie et la profondeur de l'attaque sont similaires pour tout les tubes. Le haut de chaque tube fut attaqué seulement de façon négligeable. La morphologie de cette attaque intergranulaire a été similaire à ce qui fut observé sur des alliages austénitiques exposés dans un lit fluidisé sous pression atmosphériques. On a trouvé aucune preuve que le vanadium provenant du coke "syncrude" joue un rôle dans la corrosion.

INTRODUCTION

The Mineral Sciences Laboratories (MSL) of CANMET are carrying out laboratory-scale circulating fluidized bed combustion trials of various fuels and sulphur-sorbents of interest to Canadian industry. Circulating fluidized bed combustors offer certain advantages over bubbling bed combustors, including the ability to burn fuels of low reactivity and, on a larger (electric utility) scale, better variable load characteristics. Complete details of the MSL combustor and work undertaken in it have been reported by Hamer (1).

The combustion chamber of the MSL apparatus is 2800-mm high consisting of a 150-mm diameter bottom section 610-mm high and a 100-mm diameter upper section 2190-mm high. Three horizontally mounted stainless steel tubes spanned the combustor, one each at the bottom, middle and top of the upper (100-mm diameter) section of the combustion chamber. These three tubes were 12.8-mm diameter by 0.95-mm wall thickness ASTM A213/269 Type 304 stainless steel (nominal 1/2-in. diameter by 0.035-in. wall, composition, weight % - 8.0-11.0 Ni, 18.0-20.0 Cr, 0.08 max C, 2.00 max Mn, 0.040 max P, 0.030 max S, and 0.75 max Si) and served as both uncooled corrosion specimens and pressure probes into the combustion chamber. The combustor normally operated with a nominal velocity of 3 to 3.5 ms^{-1}, a temperature of 850 to 880^{o}C, and a Ca/S ratio of 2.

The Corrosion Science Section of PMRL was asked to examine two sets of corrosion specimens, referred to subsequently as Set

1 and Set 2. Set 1 had been in the combustor during trials of "Syncrude coke" and Fort McMurray limestone. This coke is a by-product of the Syncrude Canada Ltd. tar sands plant and contains 7% sulphur plus significant quantities of vanadium. Vanadium in heavy oils is known to accelerate corrosion through the production of low melting-point phases (2). It was not known if the vanadium in the Syncrude coke would act in a similar manner. This first set of specimens was exposed for 125 h of combustor operation during 17 runs of 4.5 h or more (33 start-ups).

The second set (Set 2) of specimens was exposed for 125 h of combustor operation during 23 runs of 4.5 h or more (26 start-ups) with Minto coal (7% S) and New Brunswick limestones as feedstocks.

Both sets of specimens were at temperatures above ambient but below 850 ^{o}C during start-up and shut-down procedures for 30 to 40% longer than the 125-h "exposure" given. Analyses of fuels and limestones are given in Tables 1 and 2. Reference 1 should be consulted for additional information on the feedstocks and combustor operation.

EXAMINATION OF SAMPLES

Figures 1 and 2 show the tops and bottoms of both sets of tubes as delivered to the Corrosion Science Section. Set 1 (Fig.1), exposed to Syncrude coke, had significant deposits on the bottoms of all three tubes. The somewhat mottled appearance of the deposit, especially toward the sides of the tube,

suggested that the deposit had spalled from the sides. All three tubes had areas of uniform-appearing deposit at the bottom centre. The tops of all three tubes from Set 1 had no adherent deposit, but were covered with a relatively thin scale overlaid with a non-adherent dusty deposit.

Tubes of Set 2 (Fig. 2), exposed to the Minto coal appeared somewhat different from Set 1 in that, although the bottoms were dull red, scaled and discoloured, little deposit remained. The tops were similar to those of Set 1 and covered with a thin scale and dusty deposits.

The tubes were coated with an epoxy resin to retain scale and deposits, and a length of approximately 5 mm was cut from the centre of the hot zone of each tube. Standard procedures for metallographic specimen preparation were used for mounting and polishing the sections. Figures 3 and 4 contain photomicrographs of sections from the top and the bottom of each of the 6 tubes.

The tops of all tubes had a few minor intergranular intrusions of scale extending about 5 um into the tube. All tubes had considerable intergranular corrosion and internal attack on the bottoms where deposits or remnants of deposits were present. The attack extended over the bottom 90^{o} ($\pm$ perhaps 15^{o}) of the tube to a depth of about 70 um, corresponding to an attack rate of nearly 5 mma^{-1}. The depth of attack was more uniform on Set 1 tubes (Syncrude coke) than on Set 2 tubes (Minto coal). The maximum severity of attack was on the middle tube of Set 2 where, in one area, scale intrusion and internal precipitates of

oxides and sulphides extended up to 120 um into the specimen along grain boundaries. Metallographically there was little difference in the type of attack among the three samples from each set or between the two sets. Intergranular attack was always associated with surface deposits, or areas where there were indications that deposits had existed during combustor operation.

Only the middle tube of Set 2 appeared to have a measurable loss in wall thickness (20 or 30 um) and this occurred in the same region as the internal attack. There was no evidence of erosion of the tubes.

ELECTRON PROBE MICROANALYSES

Two samples from Set 1 and one sample from Set 2 were submitted to the Metal Physics Section of PMRL for electron-probe microanalyses. Results of these analyses are given in Fig. 5 to 11, in the form of X-ray maps for the elements of interest. Only the bottoms of the tubes (where there was significant attack) were analysed. Only Set 1 was analysed for vanadium. Results from all three specimens examined are very similar. The alloy scale and large intrusions are very rich in chromium and are probably primarily Cr_2O_3 containing significant amounts of sulphur and silicon. Further into the alloy the grain-boundary precipitates are rich in chromium, sulphur, manganese and silicon and are probably CrS and MnS, with MnS precipitates at the advancing edge of the attack zone. The Cr_2O_3 scale and many of the precipitates also contain significant amounts of Si, although

the concentration is not as high as the X-ray maps in Fig. 5 and 6 appear to indicate. The intensity of X-rays from silicon is high, and X-ray adsorption in the oxides/sulphides is lower than in the alloy. These effects lead to a spurious indication of silicon content, perhaps as much as six times the true concentration. The alloy adjacent to the grain boundaries is depleted in chromium and, therefore, appears enriched in nickel. The corrosion-product scale is covered with a deposit that is rich in calcium, but surprisingly low in sulphur. In at least one area examined (Fig. 7), no significant amount of sulphur was found in the deposit. The deposits on other specimens do contain sulphur and are expected to consist of a mixture of CaO, fuel ash constituents and $CaSO_4$. Vanadium was not found in the deposit or in the corrosion products on the samples exposed to the Syncrude coke.

DISCUSSION

There are two main findings from this investigation. First, vanadium in the Syncrude coke does not appear to cause any accelerated corrosion of Type 304 stainless steel at bed temperature in the combustion zone of a circulating fluidized bed combustor. The somewhat more uniform attack on specimens exposed to Syncrude coke is probably the result of the character of the deposit formed which may be a function of the fuel, limestone and operating conditions. As no vanadium was found in either the deposit or the corrosion products, it is difficult to believe that the vanadium content of the coke in some way influenced

deposit formation. The mechanism of formation of dense, impermeable deposits on tubes in bubbling bed FBCs is not well understood. The possible formation of low-melting-point phases (which might act as a binding agent) has been investigated, but none have been found (3). Certainly the possibility of vanadium contributing to the formation of the adherent deposit through the formation of a low-melting-point phase cannot be entirely excluded, but the lack of detectable vanadium in the deposit suggests that this is not the case. The somewhat more uniform attack on the Set 1 tubes was probably the result of deposits being retained from run to run and thus providing more constant conditions for under-deposit corrosion.

The second important result is that corrosion of Type 304 stainless steel beneath deposits in this circulating fluidized bed combustor is very similar to that observed under deposits on in-bed tubes in bubbling-bed combustors (4). It appears that the mechanism of attack in the two types of fluidized bed combustors is the same and is probably similar to that first described by Stringer and Ehrlich (5). They noted that the average activity of sulphur in most areas of a fluidized bed is not high enough to cause direct sulphidation of stainless steel. Consequently, they proposed that if a sulphate-containing deposit forms on the alloy, and if the permeability of the deposit is very low, then the activity of sulphur at the scale/deposit interface is that given by the Ca-O-S system. Calculations have shown that if local equilibrium is established between $CaSO_4$ and the alloy, the predicted phases are usually found among the corrosion products

of stainless steels exposed in FBCs.

This mechanism was developed for bubbling bed combustors where stabilized-zirconia probes show that there are regions of very low oxygen partial pressure, either because of the design of the combustor or because of the dense-phase/bubble nature of the bubbling bed. In the region of the circulating fluidized bed combustor where these tubes were exposed, there would be no dense-phase and fluctuations in the partial pressure of oxygen would be much smaller than those observed in a bubbling bed. However, the role of the deposit in restricting the access of the more oxidizing gaseous environment to the metal would be the same in both types of combustors and is, obviously, the important factor in the corrosion of the tubes in this CFBC. Where there was no deposit, there was no corrosion!

A second model for corrosion beneath deposits (discussed by Stringer and Wright (6)) postulates a reaction of CaO and the protective oxide to form an intermediate phase which is not protective. The observation from the electron-probe results that the exterior chromium-rich scale contains sulphur, calcium and silicon suggests a reaction between the Cr_2O_3 and the calcium-rich deposit. However, the model does not necessarily lead to the production of a sulphur activity at the alloy surface higher than that in equilibrium with the gaseous environment. In the case of bubbling beds, frequent excursions of the oxygen partial pressure to very low values (perhaps over 90% of the time to $pO_2 < 10^{-14}$ atm in some locations in the combustor) leads to a sulphur activity sufficiently high to cause internal sulphidation

of chromium and manganese in the alloy. However, where the tubes were located in the MSL CFBC, excursions to very low pO_2 would not be expected. Thus, it is difficult to see why a reaction between the alloy scale and the deposit would lead to sulphidation of the alloy. With sub-stoichiometric combustion conditions the pO_2 could be very low and sulphidation could occur, but in this event, sulphidation would not be restricted to the bottom of the tubes. Therefore, the occurrence of corrosion under deposits on the bottoms of the tubes in this CFBC appears to support the model of Stringer and Ehrlich.

It is difficult to judge the industrial importance of the observation that corrosion occurred under deposits in the circulating FBC. CFBCs do not have in-bed heat-transfer tubes in the combustion zone of the furnace. Water-walls are used for heat removal in the upper part of the combustor, and it is possible that deposits such as were observed on the bottoms of the tubes in the MSL combustor could form on water-walls, but the surface temperature would be much less than that of the tubes in this investigation (850^{o}C). In addition, water-walls would normally be fabricated of a carbon steel or possibly T11, not an austenitic stainless steel. Carbon steel and low-alloy ferritic steels are not susceptible to the type of attack reported here. Thermocouple wells, pressure taps and other sensor probes or ports might well be fabricated from stainless steel and operate at bed temperature and thus suffer attack. However, corrosion, or even failure, of these fittings should not be a serious problem from an operational standpoint.

CONCLUSIONS

Corrosion of Type 304 stainless steel at the temperature of the fluidized bed in a CFBC has been found under deposits on the bottoms of tubes. The rate of attack was very high, close to 5 mma^{-1}. The morphology of corrosion was similar to that observed under deposits on in-bed austenitic tubes in bubbling bed FBCs. Evidence suggests the same mechanism is responsible for the attack in both types of combustors. The sides and tops of the tubes where deposits did not form were essentially unattacked.

There was no indication that the vanadium content of the Syncrude coke accelerated corrosion.

ACKNOWLEDGEMENTS

The metallographic specimens were prepared and photographed by C. Cuzner and Y. Lafreniere of the CSS. V. Moore of the Metal Physics Section performed the electron probe microanalyses and special acknowledgement must be made to her for the excellent quality of the X-ray maps produced. M. Fichera of the CSS prepared the photo-montages and assisted in the preparation of this manuscript.

REFERENCES

1. C. Hamer and and D.T. Liang; MSL Report in preparation, 1987.

2. L.A. Morris; "Corrosion resistance of stainless steels at elevated temperatures"; Source Book on Materials for Elevated Temperature Applications; Edited by E.F. Bradley; pp 198-215, ASM, 1979.

3. J. Stringer; "Corrosion, erosion and corrosion-erosion of in-bed components in fluidized bed combustion"; Paper 90, Corrosion/86, NACE, March 1986.

4. H. Hindam, J.B. Gilmour, R.H. Packwood, D.C. Briggs and A. Lui; "The Canadian AFBC materials program - Part II; Metallographic Observations"; Paper 16, Corrosion/87, NACE, March 1987.

5. J. Stringer and S. Ehrlich; "High temperature corrosion in fluidized bed combustors"; ASME Paper 76-WA/CD-4, December 1976.

6. J. Stringer and I.G. Wright; "Materials issues in fluidized bed combustion"; J. Materials for Energy Systems 8:319-331, December 1986.

Table 1. Analyses of Syncrude Coke and Fort McMurray Limestone used in the runs with Set 1 corrosion tubes - from Hamer (1).

SYNCRUDE COKE

Proximate/Ultimate Analysis - Mass %, dry basis.

Ash	6.68
Volatile matter	6.79
Fixed C (by diff)	86.53
Carbon	82.40
Hydrogen	1.43
Sulphur	6.96
Nitrogen	2.12
Oxygen (by diff)	0.41

Calorific value 29.5 MJ/Kg

Ash Composition - Mass %

SiO_2	41.3	TiO_2	3.6
Al_2O_3	25.1	NiO	1.23
Fe_2O_3	10.9	V_2O_5	4.7
Other oxide	14.1		

FORT McMURRAY LIMESTONE - Mass %

SiO_2	13.56	MgO	0.0
Al_2O_3	3.31	SO_3	1.36
Fe_2O_3	1.43	Na_2O	0.0
TiO_2	0.34	K_2O	1.00
P_2O_5	0.14	BaO	0.10
CaO	41.23	SrO	0.02
LOI	35.15		

Table 2. Analyses of Minto Coal and New Brunswick Limestones used in runs with Set 2 corrosion tubes - from Hamer (1).

MINTO COAL

Proximate/Ultimate Analysis - Mass %, dry basis.

Ash	17.4
Volatile matter	33.7
Fixed C (by diff)	49.3
Carbon	68.3
Hydrogen	4.1
Sulphur	7.4
Nitrogen	Ø.8
Oxygen (by diff)	2.4

Calorific Value, dry, 34.6 MJ/Kg

Ash Composition, Mass %

SiO_2	28.4	CaO	4.7
Al_2O_3	9.7	MgO	Ø.2
Fe_2O_3	47.4	SO_3	4.1
TiO_2	Ø.5	Na_2O	Ø.2
P_2O_5	1.6	K_2O	Ø.4

NEW BRUNSWICK LIMESTONES - Mass %

	Havelock	Elmtree
$CaCO_3$	94.6	91.5
$MgCO_3$	1.8	1.Ø
Fe_2O_3	Ø.4	Ø.6
Al_2O_3	1.4	1.5
SiO_2	3.1	7.Ø
Na_2O	Ø.Ø3	Ø.Ø4
K_2O	Ø.2	Ø.2

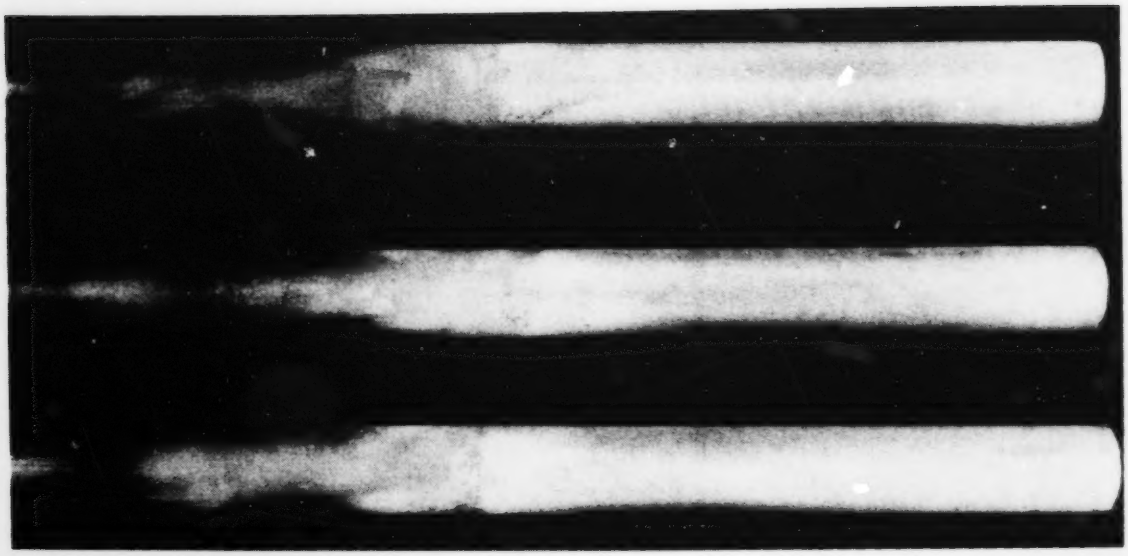

(neg 14386)

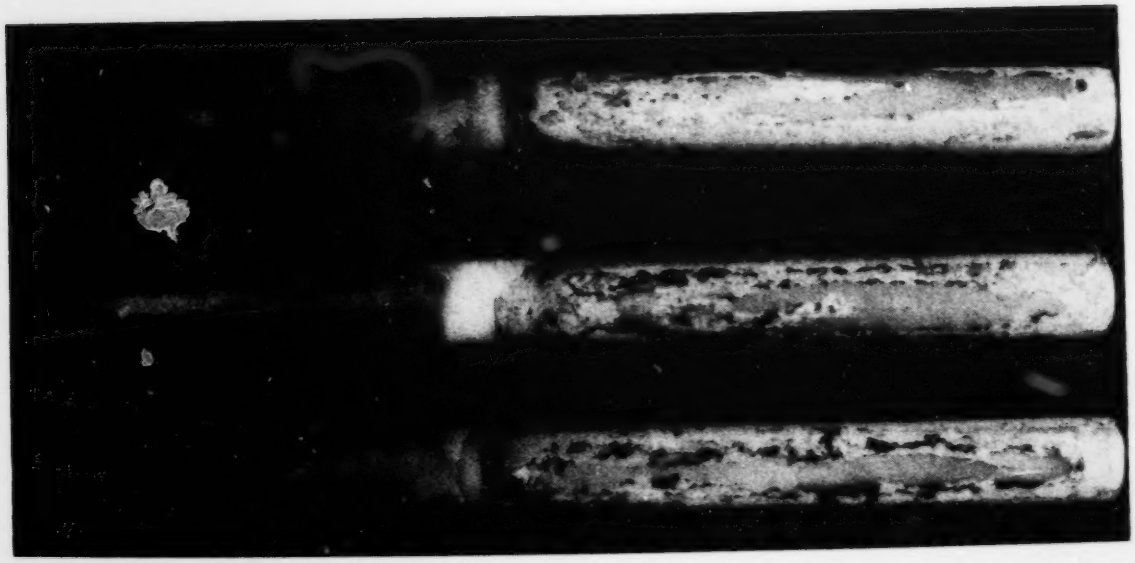

(neg 14387)

Figure 1. Photographs of the tops and bottoms of Set 1 tubes. Upper photo is of the tops of the 12.7-mm diameter tubes. T - top tube, M - middle tube, B - bottom tube.

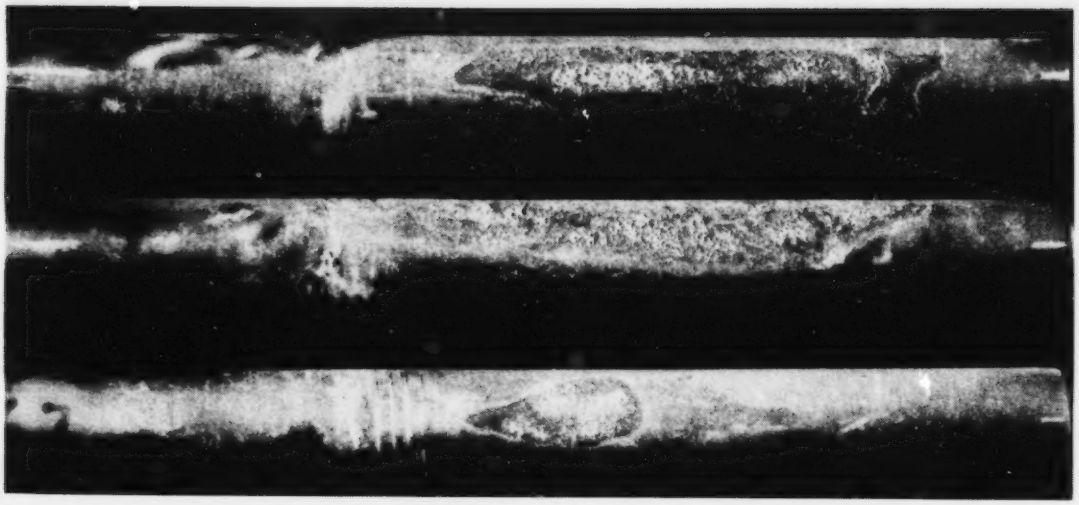

(neg 15096)

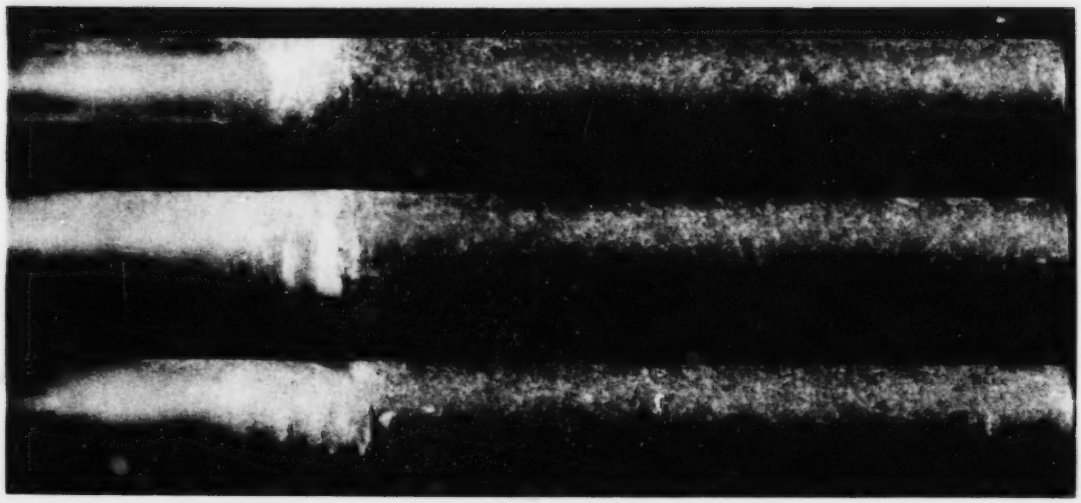

(neg 15095)

Figure 2. Photographs of the tops and bottoms of Set 2 tubes. Upper photo is of the tops of the 12.7-mm diameter tubes. T - top tube, M - middle tube, B - bottom tube.

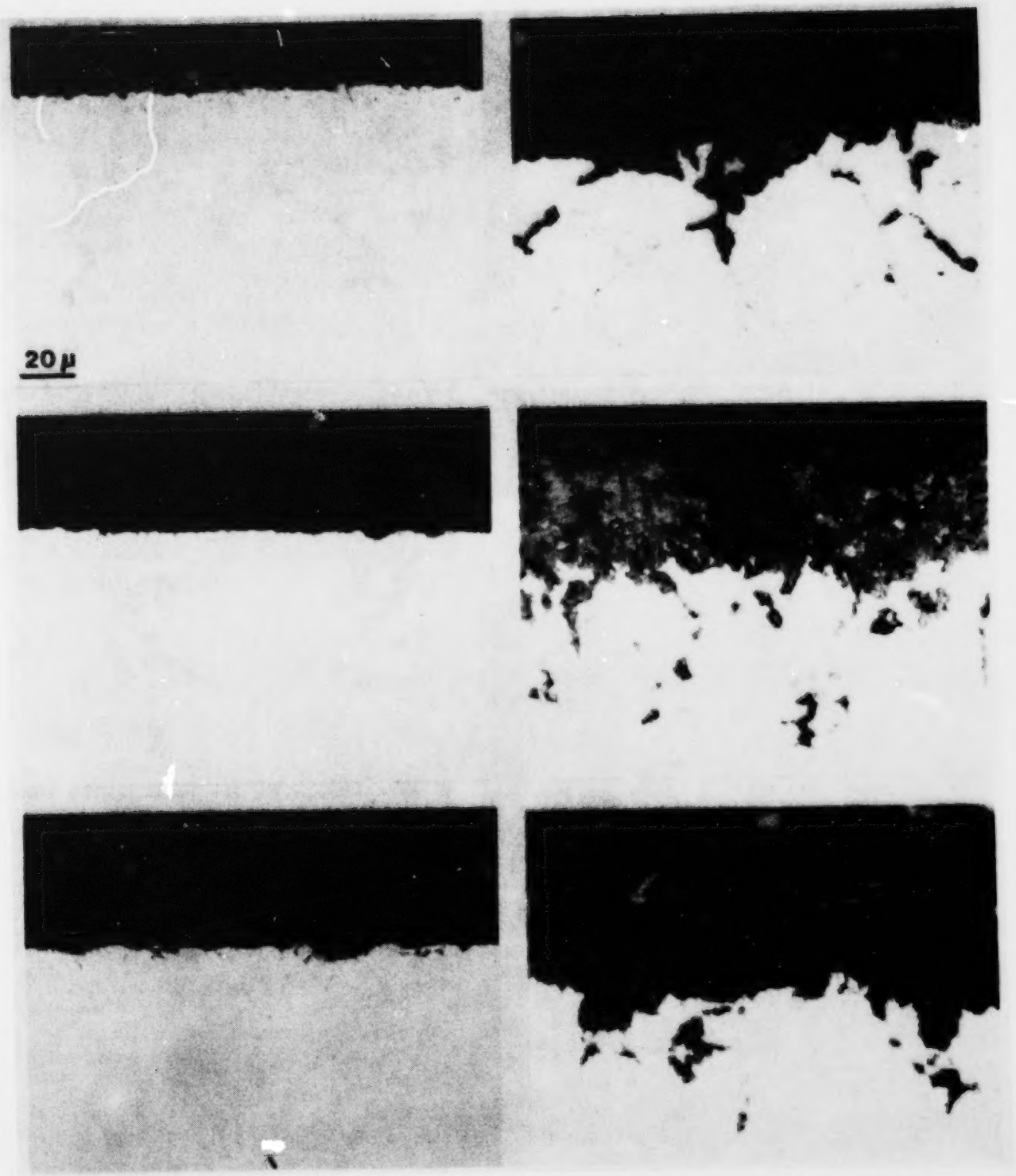

Figure 3. Photomicrographs of sections from the tops and bottoms of Set 1 tubes (Syncrude coke). The micrographs are arranged with the sections from the tops of the tubes on the left, bottoms of the tubes on the right. The top photos are the top tube and the bottom photos are the bottom tube. (neg 15338)

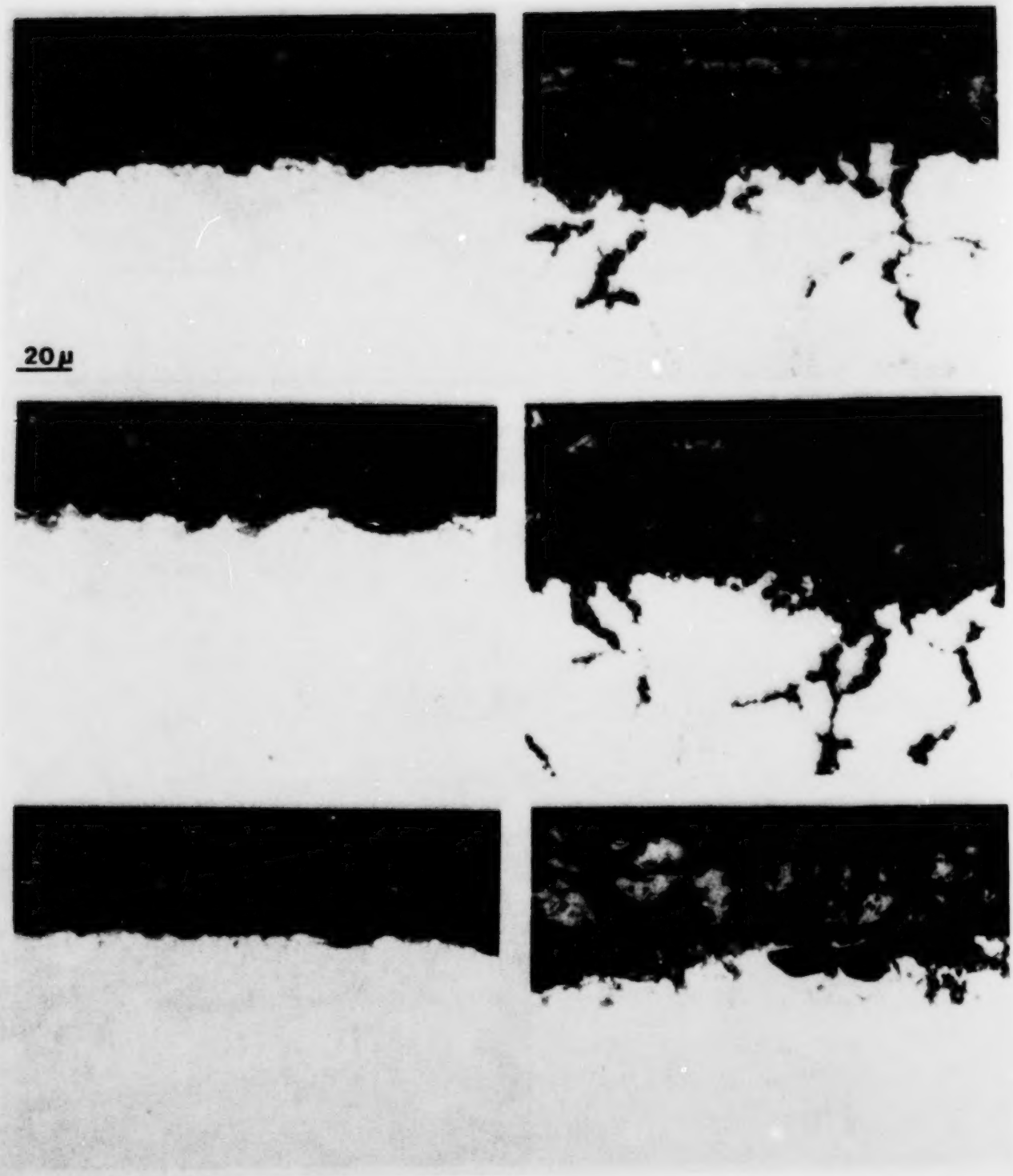

Figure 4. Photomicrographs of sections from the tops and bottoms of Set 2 tubes (Minto coal). The photographs are in the same order as those in Fig. 3. (neg 15337)

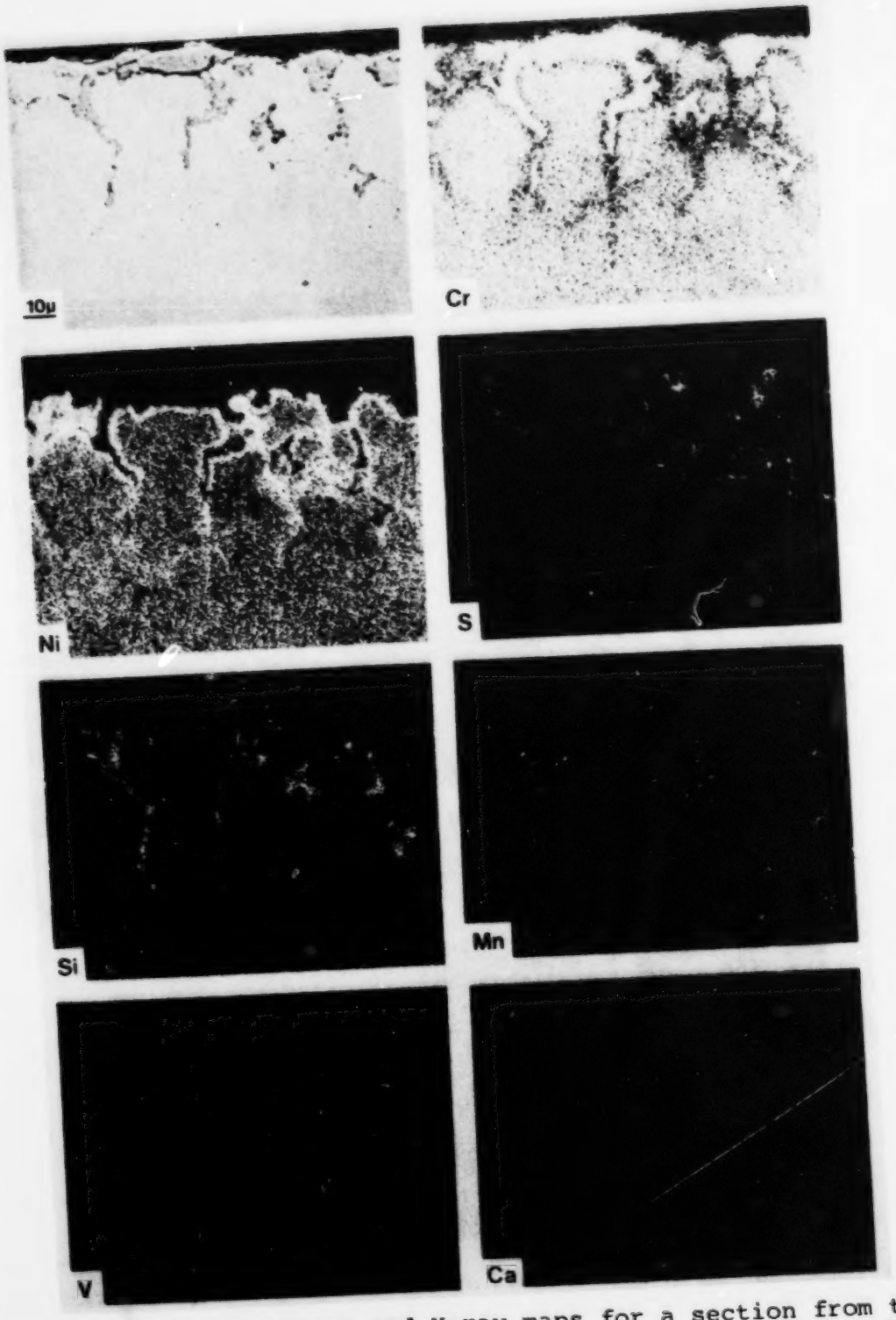

Figure 5. Electron image and X-ray maps for a section from the bottom of the bottom tube of Set 1 (Syncrude coke). (neg 15264)

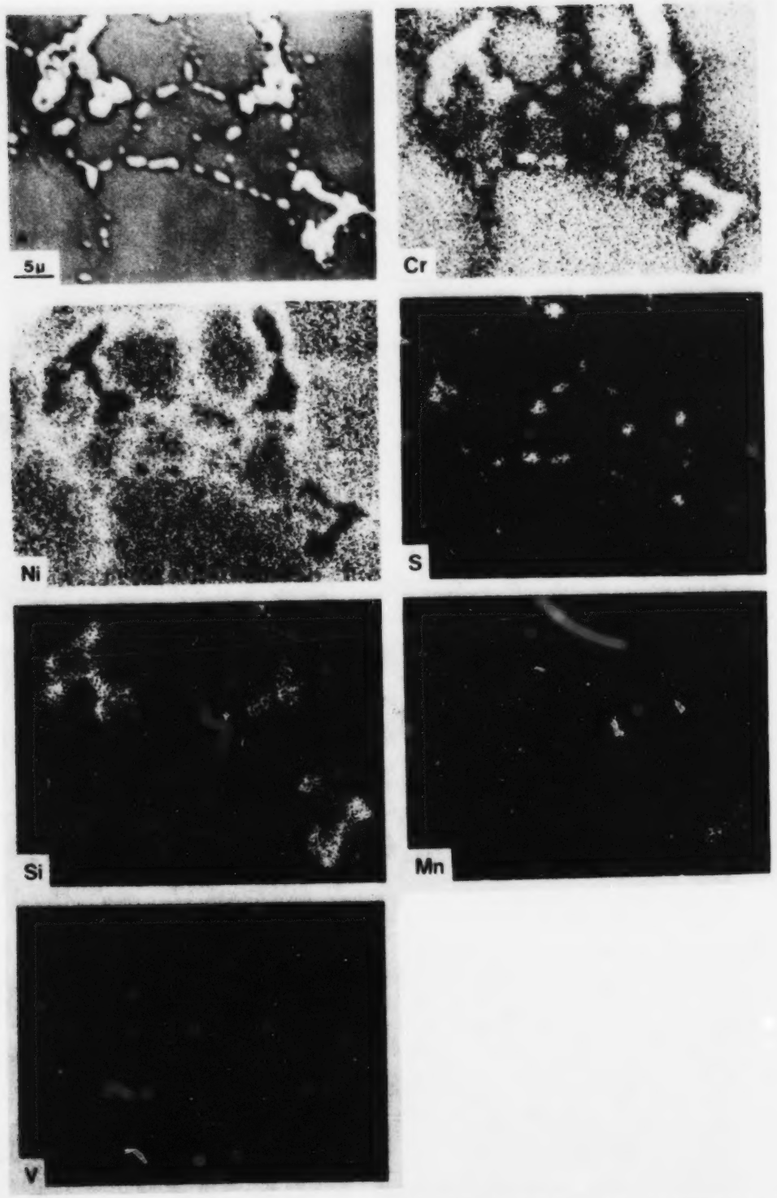

Figure 6. Higher magnification of the internally attacked area of the specimen in Fig. 5. (neg 15265)

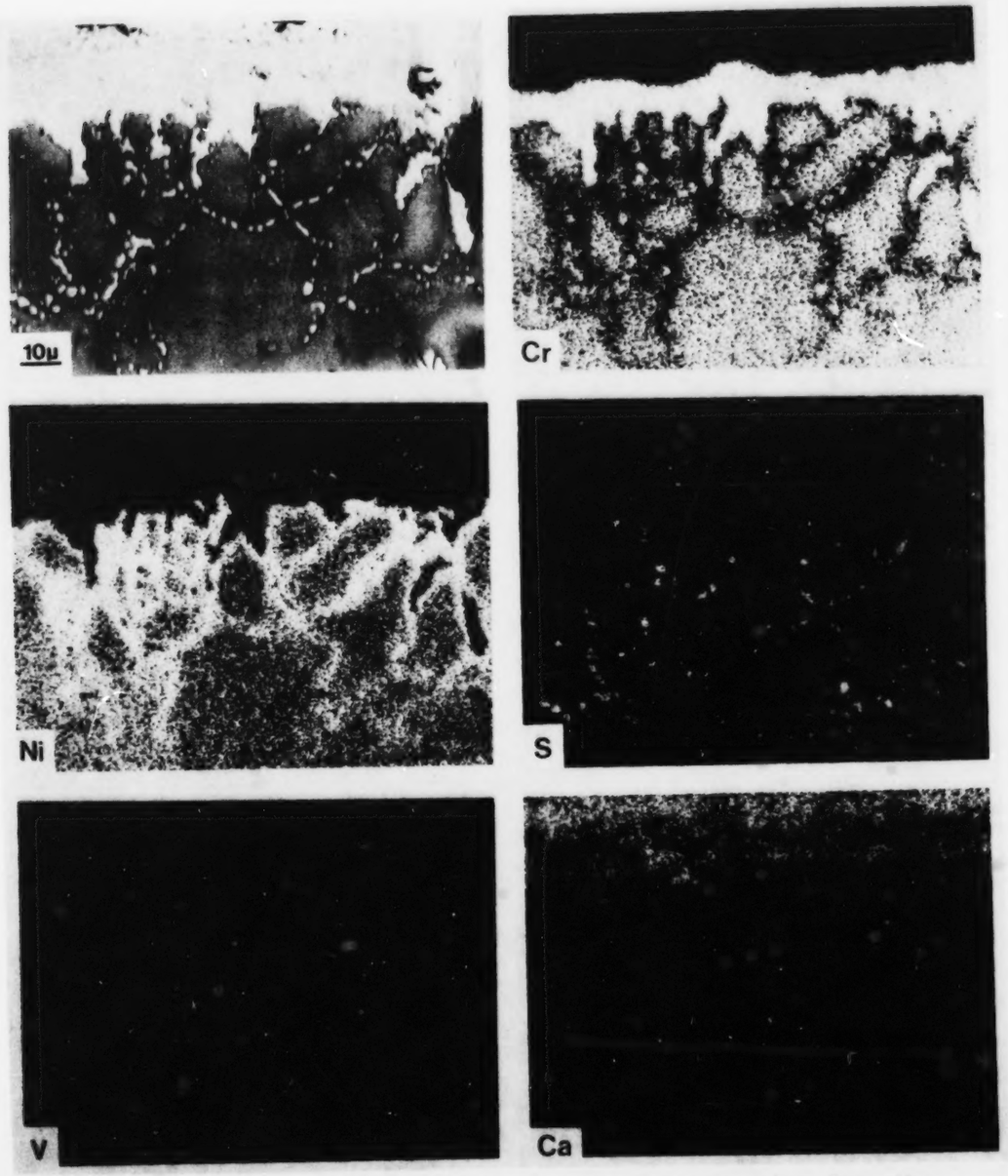

Figure 7. Electron image and X-ray maps for a section from the bottom of the middle tube of Set 1 (Syncrude coke). Note that the deposit contains Ca but little S. (neg 15267)

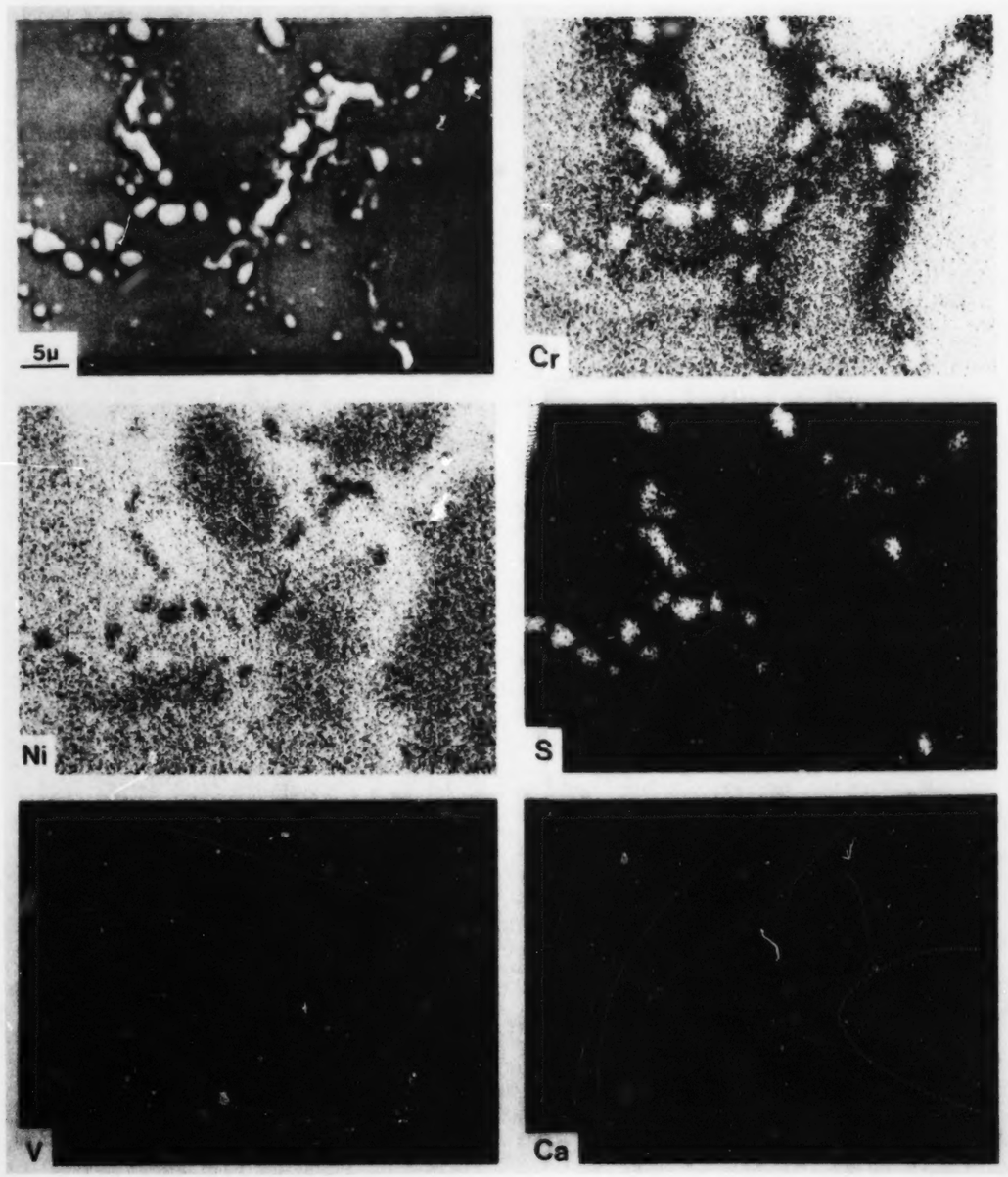

Figure 8. Higher magnification of the internally attacked area of the specimen in Fig. 7. (neg 15270)

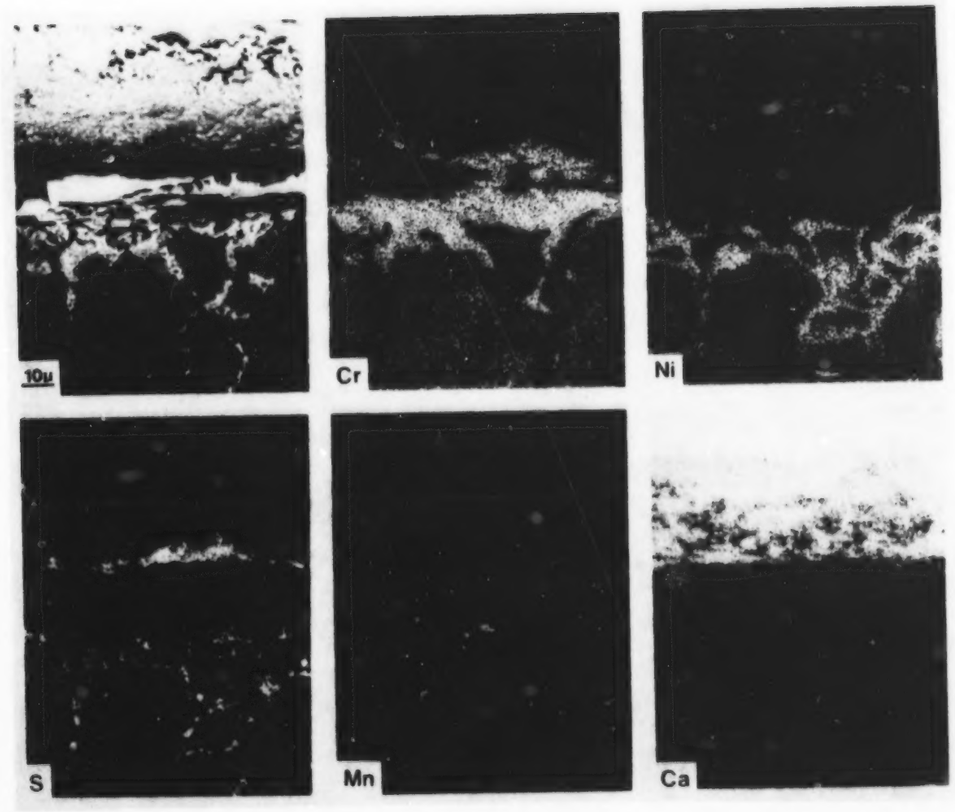

Figure 9. Electron image and X-ray maps for a section from the bottom of the middle tube of Set 1 (Syncrude coke). The deposit has separated from the scale during specimen preparation. The deposit in this section contains both Ca and S. (neg 15269)

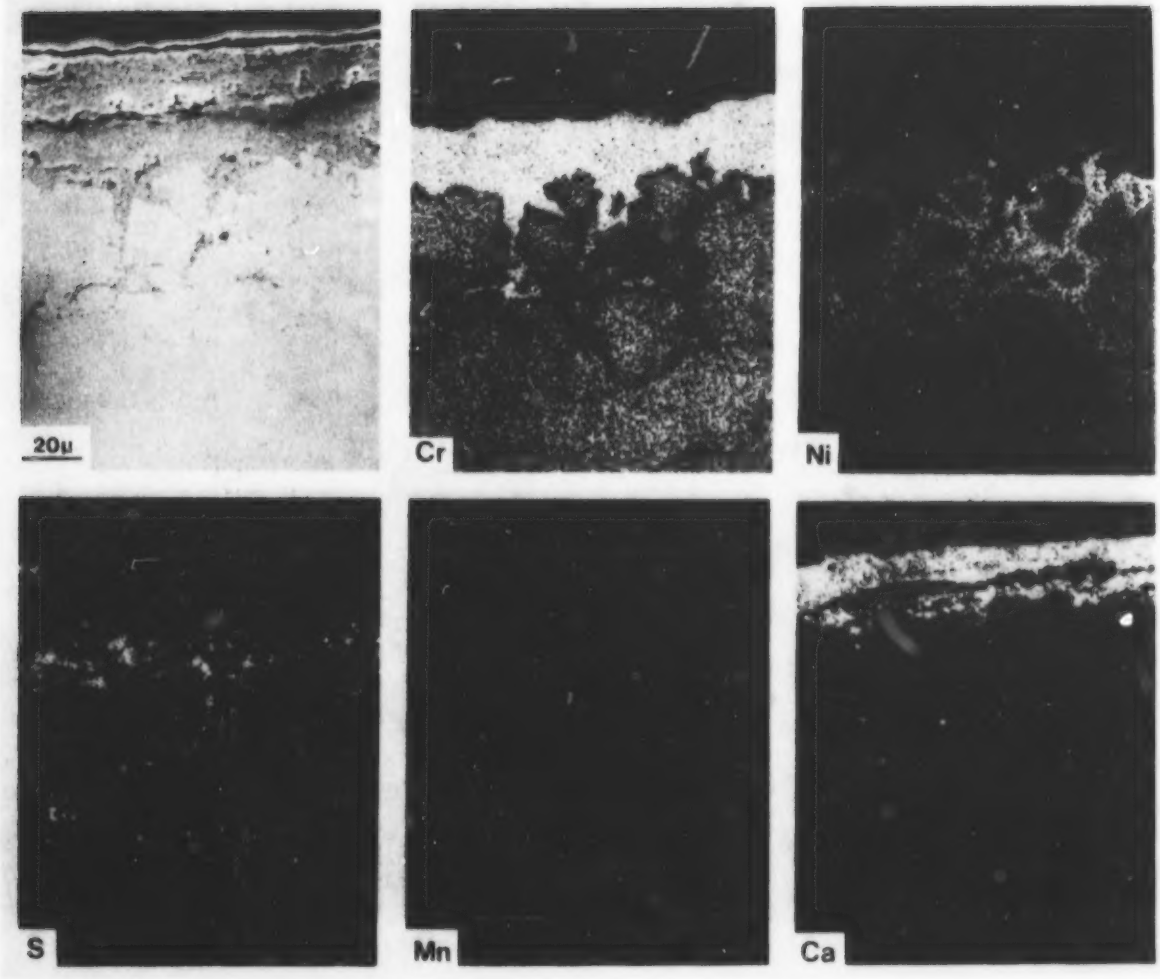

Figure 1Ø. Electron image and X-ray maps for a section from the bottom of the middle tube of Set 2 (Minto coal). The electron image is reversed contrast from those shown in the Fig. 5 to 1Ø. (neg 15266)

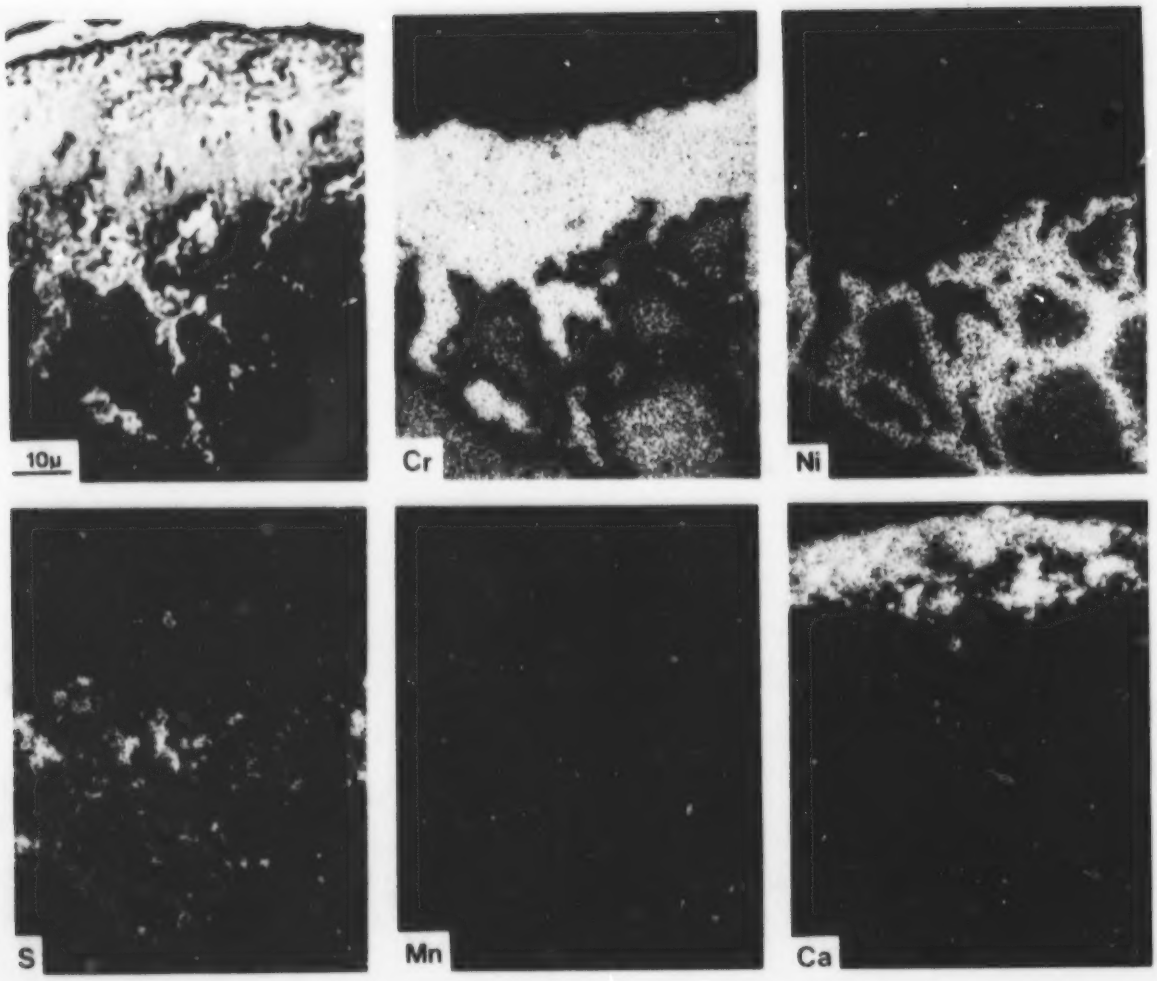

Figure 11. Electron image and X-ray maps for a section from the bottom of the middle tube of Set 2 (Minto coal). Note that this is at a higher magnification than Fig. 10. (neg 15268)